

The Influence of Thermal Deformation on the AMB-rotor System of HTR-PM Helium Circulator

Jinpeng Yu, Guowei Du, Hong Wang, Zhe Sun, and Lei Zhao

Institute of Nuclear and New Energy Technology
 Collaborative Innovation Center of Advanced Nuclear Energy Technology
 The Key Laboratory of Advanced Reactor Engineering and Safety
 Tsinghua University, Beijing, 100084, China
 yu-jp15@mails.tsinghua.edu.cn, sun_zhe@mail.tsinghua.edu.cn*

Abstract — Helium circulator is the core component of High Temperature Reactor-Pebblebed Modules (HTR-PM), and its rotor is supported by active magnetic bearings (AMBs). The windings of the motor and AMBs will generate a great deal of heat due to Ohmic loss, which increases the temperature of the circulator. The high temperature will cause the thermal deformation of AMB-rotor system, leading to the clearance change between rotor and AMBs. The AMB stiffness and inductive transducer sensitivity will be affected by the changed clearance, which decrease the stability of the AMB-rotor system. In this paper, through theoretical analysis and finite element analysis (FEA), the influence of thermal deformation on the AMB stiffness and transducer measurement is studied. The simulation and experiment for the AMB-rotor system in the circulator is carried out to explore the performance of AMB controllers and the influences of thermal deformation on the unbalanced response of the AMB-rotor system is analyzed. The theoretical calculations in this paper has general applications in the controller improvement of AMBs under clearance change and provides a reference for mechanical structure design and controller design of AMBs.

Index Terms — AMBs, HTR-PM, thermal deformation, unbalanced response.

I. INTRODUCTION

High Temperature Reactor-Pebblebed Modules (HTR-PM) is the fourth generation nuclear reactor developed by the Institute of Nuclear Energy and New Energy Technology, Tsinghua University [1, 2]. In HTR-PM, the helium circulates in the first loop driven by the circulator, which is shown in Fig. 1. The circulator is mainly composed of the rotor, active magnetic bearings (AMBs), auxiliary bearings and the cooling system. The rotor in the circulator is supported by the AMBs [3, 4]. AMBs are a type of bearing that support a load using magnetic levitation without physical

contact, and are widely applied in high-speed rotating machineries and flexible rotor-dynamic systems [5, 6]. Because AMBs have no friction and need no lubrication, its application in HTR-PM can effectively avoid the oil pollution to the helium environment in the circulator.

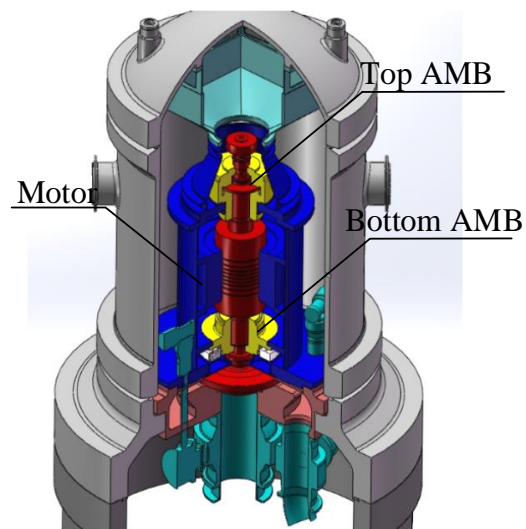


Fig. 1. 3D model of the circulator in HTR-PM.

When the circulator is running, the windings of the motor and AMBs will generate a great deal of heat due to Ohmic loss, which increases the temperature of the circulator. The components in the circulator, especially for bearings and the rotor, will deform due to the high temperature. For sliding and rolling bearings, in addition to the influence of ambient temperature, the friction between bearings and the rotor will also generate a great deal of heat, which aggravates the deformation of bearings and the rotor.

The main influence of thermal deformation is causing the clearance change between bearings and the rotor, which has influence on the dynamic performance of the bearing-rotor system. As for sliding and rolling

bearings, clearance change will affect the contact force between bearings and the rotor and change the system mode. However, clearance change affects the AMB-rotor system in different ways. AMBs are open-loop unstable systems, so the rotor position must be accurately measured by displacement transducers in real time to achieve closed-loop feedback control. Therefore, in the AMB-rotor system, the thermal deformation will not only change the AMB-rotor clearance but also the displacement transducer-rotor clearance. Since the electromagnetic force of AMBs and the voltage signals of displacement transducers are all related to the clearance, the clearance change will directly affect the performance of the AMB controller and the stability of the AMB-rotor system [7, 8].

In this paper, the influence of thermal deformation on the unbalanced response of the AMB-rotor system is studied, which provides a reference for the mechanical design of AMBs. Section II introduces and calculates the electromagnetic force of AMBs, and explores the influence of the clearance change on the AMB stiffness. The principle of inductive transducers and the influence of clearance change on the transducer measurement are analyzed. In Section III, the finite element analysis (FEA) of the circulator and transducer is carried out, and based on which the AMB-rotor system is simulated in MATLAB Simulink. Combined with theoretical analysis and FEA results, the influences of thermal deformation on the unbalanced response of the AMB-rotor system is analyzed in the experiment.

II. ANALYSIS OF THE INFLUENCE OF THE CLREANCE CHANGE

A. Influence on the AMB stiffness

In this section, the influence of the clearance change caused by thermal deformation on the electromagnetic force and AMB controller is calculated and discussed.

The AMB-rotor system is nonlinear, so it is necessary to linearize the electromagnetic force at an equilibrium point of the AMB-rotor system to simplify the AMB model and controllers design. Therefore, both the electromagnetic force and the AMB stiffness has the relationship with the clearance in the AMB-rotor system.

In a radial AMB of the circulator, as is shown in Fig. 2, there are four electromagnets (an electromagnet is composed of four magnetic poles) arranging in a ring and a pair of electromagnets in opposite directions control one degree of freedom of the rotor. Therefore, the electromagnetic force in one degree of freedom is [9, 10]:

$$F = \frac{1}{4} \mu_0 N^2 A_0 \left(\frac{(i_0 + i_x)^2}{(s_0 - x)^2} - \frac{(i_0 - i_x)^2}{(s_0 + x)^2} \right), \quad (1)$$

whose parameters are shown in Table 1.

Equation (1) can be linearized at $i_x = 0$ and $x = 0$

by Taylor expansion. Ignoring higher-order items, Equation (1) can be rewritten as:

$$F = k_x x + k_i i, \quad (2)$$

where $k_x = \mu_0 N^2 A_0 i_0^2 / s_0^3$ is the force-displacement stiffness and $k_i = \mu_0 N^2 A_0 i_0 / s_0^2$ is the force-current stiffness, all of which are directly related to the clearance s_0 .

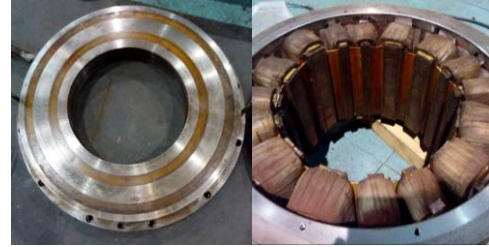


Fig. 2. A radial AMB in the circulator.

Table 1: Parameters of the electromagnetic force

Parameter	Meaning
μ_0	Magnetic permeability
A_0	Magnetic pole area
N	Coil number
s_0	Clearance
i_0	Bias current
x	Rotor displacement
i_x	Control current

When the circulator is running, AMBs and the rotor will deform due to the high temperature. The thermal deformation will cause the clearance change between AMBs and the rotor, so the notation s_0 can be rewritten as:

$$s = s_0(1 + \Delta s), \quad (3)$$

where Δs is the change of clearance and s is the clearance after thermal deformation. Therefore, the relationship between the variation ratio of the k_x , k_i and Δs is:

$$\begin{cases} \Delta k_x = [k_x(s) - k_x(s_0)] / k_x(s_0) \\ \quad = 1 / (1 + \Delta s)^3 - 1 \\ \Delta k_i = [k_i(s) - k_i(s_0)] / k_i(s_0) \\ \quad = 1 / (1 + \Delta s)^2 - 1 \end{cases} \quad (4)$$

Figure 3 shows the change of Δk_x and Δk_i when Δs varies from -0.1 mm and 0.1 mm. As the clearance decreases, Δk_x and Δk_i become larger and vice versa. And Δk_x is more sensitive to the clearance than Δk_i . In the AMB-rotor system, the stiffness k_x and k_i are constant parameters in the AMB controller. Therefore, the clearance change caused by thermal deformation eventually change the AMB stiffness, which will affect the performance of the AMB controller and the stability of the AMB-rotor system.

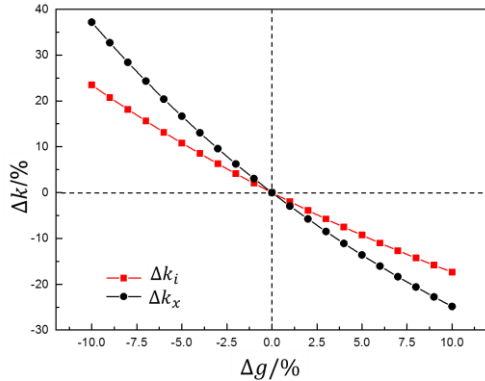


Fig. 3. The relationship between Δk_x , Δk_i and Δs .

B. Influence on the transducer sensitivity

AMBs are open-loop unstable systems, so the rotor position must be accurately measured by displacement transducer in real time to achieve closed-loop feedback control. Inductive transducers and eddy current displacement sensors are widely applied to the AMB system with their characteristics of high precision and non-contact measurement [11, 12]. In the AMB-rotor system of the circulator, differential inductive transducer is used to monitor the axis orbit of the rotor and provide feedback signal for the AMB controller.

The magnetic field generated by transducer coils will pass through transducer cores (stator), the rotor and the air-gap between the rotor and stator to form a closed magnetic circuit. The coil inductance will be affected by the air-gap length. Therefore, by measuring electrical parameters of the transducer circuit, the coil inductance can be measured, and then the rotor displacement can be obtained.

Ignoring the magnetic flux leakage and magnetic hysteresis, the magnetic circuit can be calculated:

$$\Phi = \frac{NI}{R}, \quad (5)$$

with Φ the magnetic flux, N the total coil number, I the coil current and R the reluctance. The relationship between Φ and the coil inductance L is:

$$N\Phi = LI, \quad (6)$$

and the reluctance is:

$$R = \frac{2\delta}{\mu_0 B_0}. \quad (7)$$

μ_0 is the permeability of vacuum, δ is the air-gap length and B_0 is magnetic pole area of the transducer. So according to Equations (5), (6) and (7), the coil inductance is:

$$L = \frac{N^2 \mu_0 B_0}{2\delta}. \quad (8)$$

Similar to AMBs, two transducers in opposite directions measure δ_1 and δ_2 in one direction to obtain the rotor displacement, which is the differential measurement, as is shown in Fig. 4. Therefore, the

clearance is $s_0 = (\delta_1 + \delta_2)/2$ and the rotor displacement is $x = (\delta_1 - \delta_2)/2$. In the measurement, a resistance-balanced bridge circuit is applied to convert the inductance into a voltage output, which is transmitted to the AMB controller.

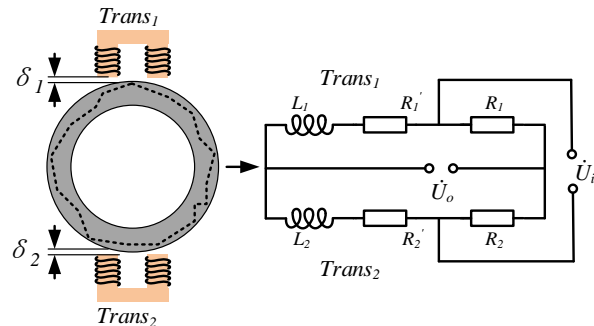


Fig. 4. Differential measurement and the resistance-balanced bridge circuit for transducer measurement.

The output voltage of the circuit is:

$$\begin{aligned} \dot{U}_o &= \frac{Z_1}{Z_1 + Z_2} \dot{U}_i - \frac{R_1}{R_1 + R_2} \dot{U}_i \\ &= \frac{Z_1 - Z_2}{2(Z_1 + Z_2)} \dot{U}_i, \end{aligned} \quad (9)$$

where $Z_i = j\omega L_i + R_i'$ ($i = 1, 2$) is the impedance of the transducer coils under alternating currents, R_i' ($i = 1, 2$) is the coil resistance, R_i ($i = 1, 2$) is the balancing resistance, \dot{U}_i and \dot{U}_o are the input and output voltage respectively. Ignoring the coil resistance, the relationship between the output voltage and rotor displacement can be obtained according to Equations (8) and (9):

$$\dot{U}_o = \frac{x}{2s_0} \dot{U}_i. \quad (10)$$

It can be seen that the output voltage of the transducer is proportional to the rotor displacement. During designing the AMB controller, transducers need to be calibrated to obtain the transducer sensitivity, which is the relationship between the sensor output voltage and the actual rotor displacement:

$$\xi_0 = \frac{\dot{U}_o}{x} = \frac{\dot{U}_i}{2s_0}. \quad (11)$$

As shown in Equation (11), the transducer sensitivity ξ_0 is directly related to the clearance s_0 . Therefore, according to Equations (3) and (11), if the clearance changes, the error caused by the sensor sensitivity is:

$$\eta = \frac{\xi}{\xi_0} - 1 = \frac{1}{(1 + \Delta s)} - 1. \quad (12)$$

In the AMB controller, the transducer sensitivity is a constant parameter. Therefore, Equation (12) shows that once the thermal deformation changes the transducer-rotor clearance, the transducer sensitivity and the measurement accuracy of rotor displacement will be affected, which will reduce the performance of the AMB controller AMB-rotor stability.

III. FEA OF THE CIRCULATOR SYSTEM

A. Temperature-deformation coupled FEA for the circulator

To obtain the temperature field and thermal deformation of the circulator, the circulator model is built and analyzed in ANSYS using temperature-deformation coupled FEA. The model material is the mild steel whose parameters are shown in Table 2. The coefficients of thermal deformation, thermal conductivity and specific heat capacity can be obtained from Figs. 5-7.

Table 2: The material parameters of the mild steel

Material Parameter	Unit	Value
Density	t/mm ³	7.85e-9
Young's modulus	MPa	210000
Poisson's ratio	-	0.26
Thermal deformation	1/°C	Fig. 5
Thermal conductivity	J/mm°Cs	Fig. 6
Specific heat capacity	J/t°C	Fig. 7

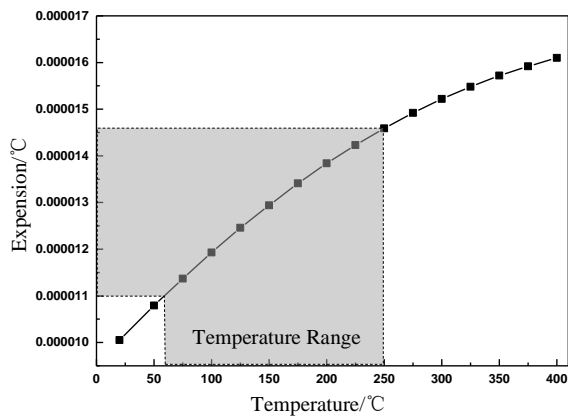


Fig. 5. Relationship between the thermal deformation and the temperature.

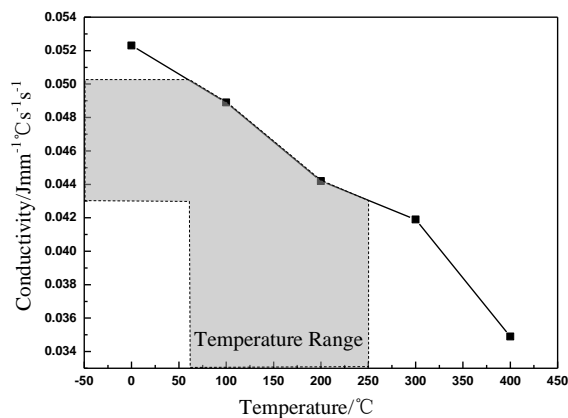


Fig. 6. Relationship between the thermal conductivity and the temperature.

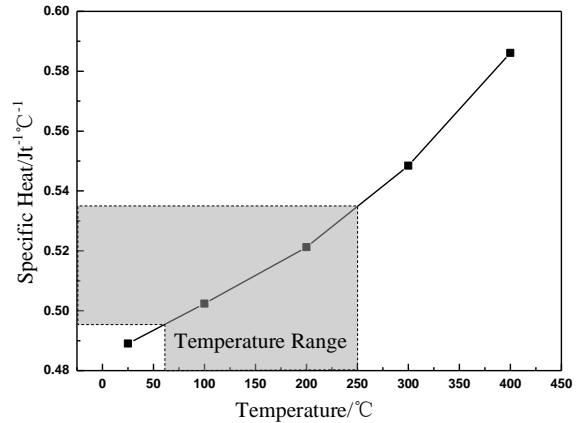


Fig. 7. Relationship between the specific heat capacity and the temperature.

The circulator model is built as shown in Figs. 1 and 8. In the FEA, the bottom of the rotor and housing constrained the freedoms of X, Y and Z directions, and the top of the rotor constrained the freedoms of X and Z directions. The original clearance s_0 is 1 mm.

The actual size model is used for simulation. Since the structure of the circulator is simple and there are no complicated components, the adaptive algorithm is used for automatic meshing. In the FEA of temperature field, stable heat sources are applied to the circulator to simulate the heat source caused by the windings of the motor, AMBs and the heat transferred by the high-temperature helium gas through the circulator components. Parameters of heat sources are obtained based on the data measured by the temperature sensor in the experiment.

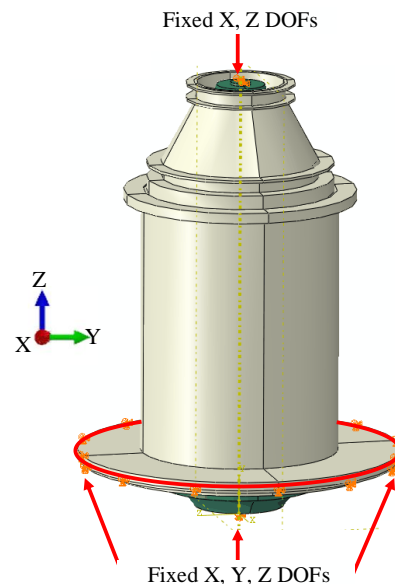


Fig. 8. The circulator model for FEA.

A forty-minute stable operation is simulated, at the beginning of which the rotor speed increase from 0 rpm to 3200 rpm. The temperature of the different components in the circulator gradually rises from 25 degrees Celsius to a steady value. The steady temperatures at different positions are listed in Table 3 and the temperature field is shown in Fig. 9.

Table 3: The steady temperatures at different positions

Position (From Top to Bottom)	Temperature/°C
Top part of auxiliary impeller	62.4
Bottom part of auxiliary impeller	69.0
Axial bearings	67.1
Top radial bearing	64.7
Top part of motor chamber	78.3
Motor winding	73.5
Bottom part of motor chamber	69.7
Bottom radial bearing	73.0
Outer surface of motor housing	65.0
Impeller chamber	250.0

It can be seen from the FEA results, that the heat from the motor and AMBs lead to the thermal deformation of the rotor and stator. Due to different geometrical dimensions, material properties and different stable temperature, the rotor and stator have different deformation ratios, which leads to clearance change of AMBs and transducers (both in the top and bottom radial AMBs). The thermal deformation of the structure can be obtained as shown in Fig. 10.

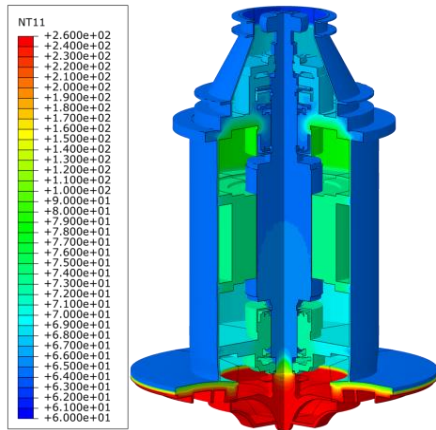


Fig. 9. The stable temperature field of the circulator.

The expansion of the stator is greater than the rotor, so the clearance is increased. It shows that the clearance increases 4.3% in the top radial AMB and 5.12% in the bottom radial AMB. The inconsistency of the clearance change in the top and bottom AMBs is because the high-temperature helium gas. When the circulator is running, the bottom AMB is close to the high-temperature helium

gas, so it has a larger clearance change under higher temperature.

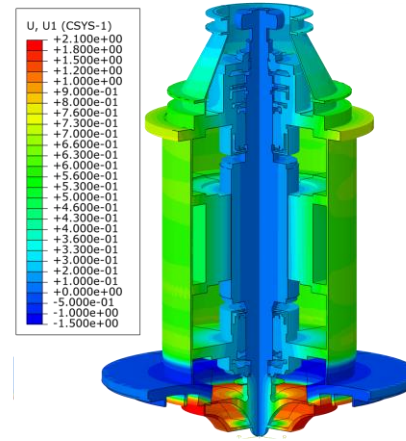


Fig. 10. The thermal deformation of the circulator

According to the calculation and analysis of Section II, the increasing clearance reduces the AMB stiffness and transducer sensitivity, which are listed in Table 4.

Table 4. The parameter variation

Top		Bottom	
Δs_t	4.3%	Δs_b	5.1%
Δk_{x_t}	-11.9%	Δk_{x_b}	-13.9%
Δk_{i_t}	-8.1%	Δk_{i_b}	-9.5%
η_t	-4.1%	η_b	-4.9%

B. Electromagnetic field FEA for the inductive transducer

Based on the clearance change calculated in the Section III (A), the electromagnetic field FEA is carried out to explore the influence of clearance change on inductive transducers.

The 3D model of the inductive transducer is built as shown in Fig. 11. Since the transducer use differential measurement in the circulator, the inductance of upper and lower transducers is calculated in FEA. The FEA is carried out with the rotor displacement of +0.1 mm in vertical direction. The clearance is obtained in Section III (A). The original clearance is $s_0 = 1$ mm, and the clearance change is $\Delta s_t = 4.3\%$ in the top radial AMB and $\Delta s_b = 5.1\%$ in the bottom radial AMB.

In the model, the rotor and stator are assembled with silicon steel sheets to reduce the effects of eddy current. Because the mechanical design of the model is simple and there are no complicated structural components, the adaptive algorithm is used to automatic meshing. The inductive transducer uses an alternating current (AC) excitation source, so the current in the coils is 20 KHz in the simulation. The simulation runs for one cycle of the excitation source in every project.

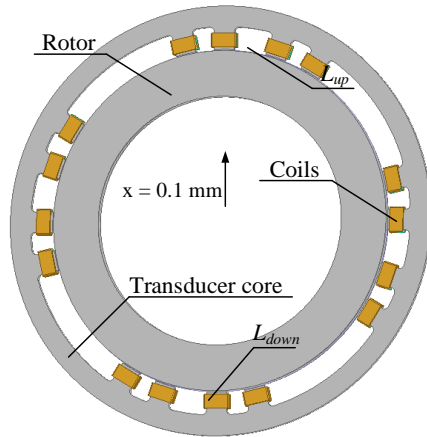


Fig. 11. 3D model of the inductive transducer.

The results of magnetic flux density in FEA are shown in Fig. 12. The picture shows the electromagnetic field distribution in the silicon steel sheets (transducer and rotor) when the current is maximum. With the same rotor displacement, the magnetic field changes significantly due to the clearance change, which directly affects the calculation of the transducer inductance.

It can be seen from the results that the increase of the clearance increases the magnetic resistance of the inductive transducer, which reduce the magnetic induction intensity inside the rotor and the stator and reduce the inductance value. The results are consistent with the analysis in Section II.

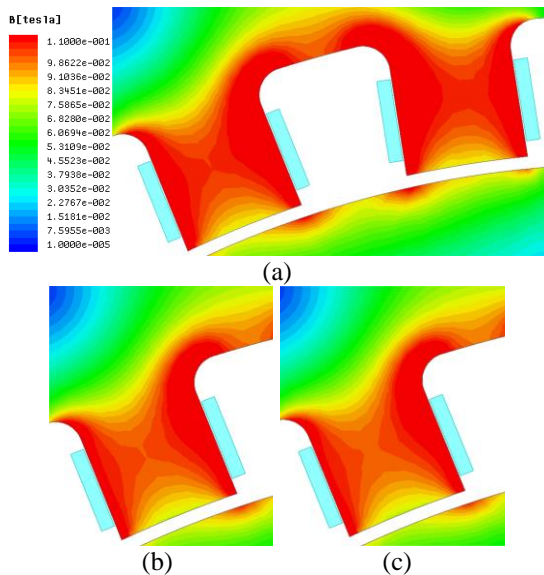


Fig. 12. The magnetic flux density in the transducer: (a) the original clearance $s_0 = 1$ mm, (b) $\Delta s_t = 4.3\%$ in the top AMB, and (c) $\Delta s_b = 5.1\%$ in the bottom AMB.

Because the transducer inductance can be obtained easily, the measurement error caused by the sensor sensitivity can be substituted by:

$$\sigma = \frac{x}{s_0}, \quad (13)$$

which has the same changing trend with η . According to FEA results and Equations (8), (12) and (13), the transducer inductance and measurement error are shown in Table 5. Due to the clearance change, the transducer sensitivity changes significantly, leading to measurement error of the rotor displacement. The measurement error in the top AMB is -4.31% and the bottom is -4.87% , which are consistent with the theoretical calculation in Table 4.

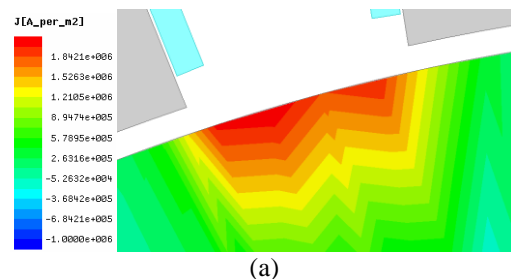
Table 5: The transducer inductance and measurement error

s (mm)	L_{up} (mL)	L_{down} (mL)	σ (%)	η (%)	
s_0	1.0	0.0658	0.0565	7.604	0.00
$s_0 + \Delta s_t$	1.043	0.0634	0.0548	7.276	-4.31
$s_0 + \Delta s_b$	1.051	0.0630	0.0545	7.234	-4.87

According to the simulation results, the AC excitation source of the inductive transducer leads to the changing magnetic induction intensity, which generates the eddy current in the rotor, as shown in Fig. 13. According to reference [13], the eddy current also affects the measurement accuracy of the inductive transducer. As shown in the Table 6, due to the change of the clearance, the maximum Eddy current density on rotor surface is significantly increased, which will further affect the measurement accuracy of the transducer. However, due to the complex relationship between the distribution of the eddy-current magnetic field and the rotor speed, the calculation is difficult and further theoretical analysis is needed.

Table 6. The Eddy current on the rotor surface.

s (mm)	J_z (A/m ²)	
s_0	1	-8.317e+5
$s_0 + \Delta s_b$	1.051	-8.680e+5
$s_0 + \Delta s_t$	1.043	-8.684e+5



(a)

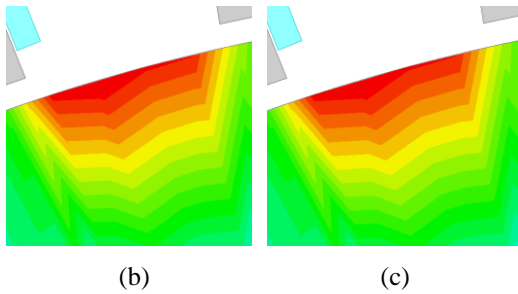


Fig. 13. The eddy current density in the transducer: (a) the original clearance $s_0 = 1 \text{ mm}$, (b) $\Delta s_t = 4.3\%$ in the top AMB, and (c) $\Delta s_b = 5.1\%$ in the bottom AMB.

IV. UNBALANCED RESPONSE OF THE AMB-ROTOR SYSTEM UNDER THERMAL DEFORMATION

A. Simulation of the AMB-rotor system

Due to the material inhomogeneity and machining error, the rotor possesses unbalanced mass inevitably, which will cause unbalance force for the rotor. When the circulator is running, the rotor unbalanced vibration caused by the unbalanced force will increase with the increasing rotor speed, but the AMB controller will suppress the rotor unbalanced vibration via active electromagnetic force [14-16]. However, the AMB controller is designed based on the original AMB-rotor system, which means the clearance change will change the controller parameters and affect the unbalanced response of the AMB-rotor system. In this section, the simulation of AMB-rotor system is carried out to study the influence of thermal deformation on the unbalanced response of the AMB-rotor system.

Based on the FEA of the thermal deformation and transducer measurement, the AMB-rotor system in circulator is built and simulated in MATLAB Simulink, as is shown in Fig. 14. The system includes the rotor module that considers the gyroscopic effect and unbalanced mass, the cross-feedback module, and the AMB controller module. The system is under cross-feedback PID control and the rotor speed is 60 Hz. Based on the data in Table 4, change the parameters of the system and runs the simulation.

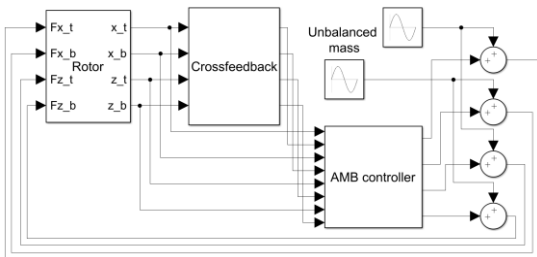


Fig. 14. The AMB-rotor system in circulator.

In the simulation, the rotor speed increase from 0 to 60 Hz and runs stably. The unbalanced vibration of the rotor is simulated by applying a periodic external force at F_{x_t} and F_{x_b} . The output of x_t and y_t compose the axis orbit of the top AMB, and x_b and y_b compose the bottom. The clearance change is simulated by changing the force-displacement coefficient and force-current coefficient of the AMB and the transfer coefficient of the transducer.

The axis orbits of the rotor at the top and bottom AMBs are shown in Fig. 15, where the horizontal axis represents the rotor displacement in the X direction and the vertical axis represents Z direction. The solid blue line and red dotted line are the axis orbits of the rotor in original clearance and changed clearance, respectively.

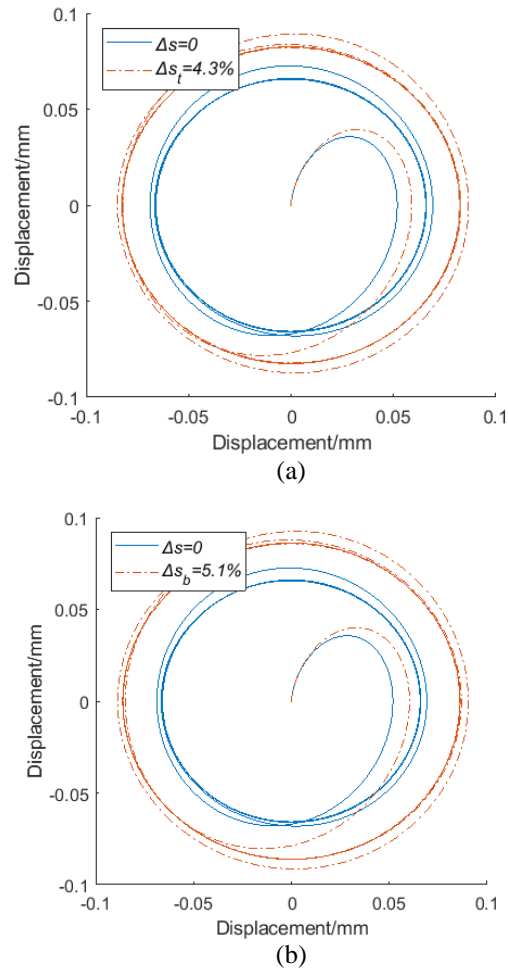


Fig. 15. Axis orbit of the rotor under different clearance change: (a) top AMB and (b) bottom AMB.

Under the influence of the unbalanced mass, the rotor vibrates when the rotor speed is fixed. However, after the thermal deformation, the clearance change leads

to the axis orbit expand both in the top and bottom AMB. The results show that the clearance change will reduce the performance of the AMB controller and aggravate the rotor vibration.

B. Operation experiment of the circulator

The experiment for circulator is carried out to explore the performance of AMB controller and stability of AMB-rotor system under high temperature environment. In the experiment, the rotor speeds up to 3200 rpm in 7 min and the axis orbit of the rotor is obtained at time A. After the circulator temperature is stable, the axis orbit of the rotor at time B is recorded. The temperatures at different position of the circulator are measured by the temperature sensor, which are the reference of the heat sources in the FEA.

Figure 16 shows the experimental result. The vertical axis on the left shows the ratio of the radial vibration amplitude to clearance and the right one shows the rotor speed. It can be seen that the rotor speed can be well controlled. Before 7 min, the vibration amplitude of the rotor increases as the rotor speeds up. This is due to the unbalanced force resulting from the unbalanced mass of the rotor. The unbalanced vibration is proportional to the rotor speed, but when the rotor speed is fixed at 3200 rpm after 7 min, the vibration amplitude of the rotor continues to increase. At this point, the factor that affect the vibration amplitude is not the rotor speed, but the clearance change caused by the thermal deformation.

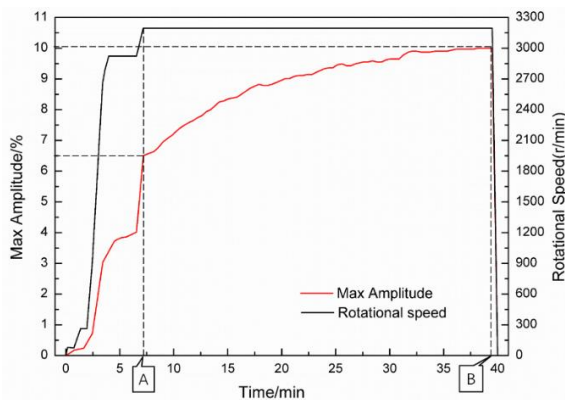


Fig. 16. Rotor speed and vibration amplitude.

In Figs. 17 and 18, the horizontal and vertical axis represents the rotor displacement. It can be seen that at time A, the axis orbit and the vibration amplitude of the rotor is small, while at time B, the vibration amplitude significantly increases.

The experimental results show that with a fixed rotor speed, the vibration amplitude of the rotor gradually increases with the increasing temperature of the circulator. And when the temperature is stable, the vibration amplitude of the rotor tends to be stable. The

experiment shows that the unbalanced vibration of the rotor increases with the increasing temperature of the circulator after long-term operation. The thermal deformations affect the clearance, and then reduce the performance of the AMB controller and affect the unbalanced response of the AMB-rotor system. This is consistent with theoretical analysis and simulation.

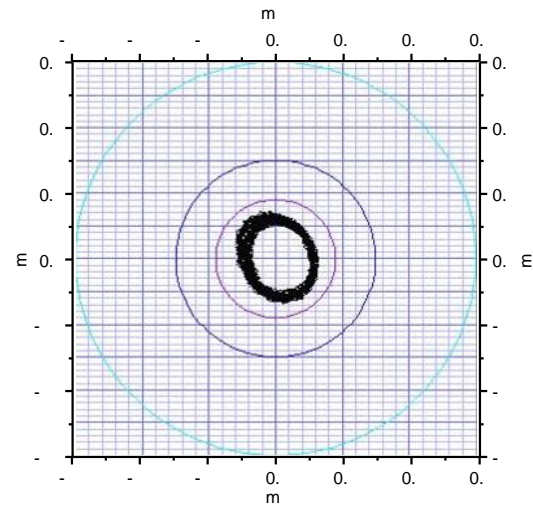


Fig. 17. Axis orbit of the top AMB at time A.

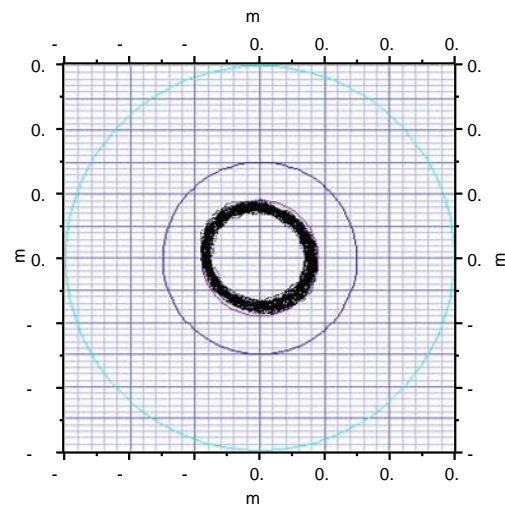


Fig. 18. Axis orbit of the top AMB at time B.

V. CONCLUSION

In this paper, the influence of thermal deformation on the unbalanced response of the AMB-rotor system is studied, which provides a reference for the mechanical design of AMBs.

According to the theoretical analysis, clearance change caused by thermal deformation eventually change the AMB stiffness. As the clearance decreases, Δk_x and Δk_i become larger and vice versa. And Δk_x is

more sensitive to the clearance than Δk_i . The thermal deformation will also change the transducer-rotor clearance, and the transducer sensitivity and the measurement accuracy of rotor displacement will be affected, which lead to the measurement error of the rotor displacement.

From the FEA results, the heat from the motor and AMBs contribute to the deformation of the circulator. The clearance increases 4.3% in the top radial AMB and 5.12% in the bottom radial AMB. Due to the clearance change, the transducer sensitivity changes significantly, leading to measurement error of the rotor displacement. The measurement error in the top AMB is -4.31% and the bottom is -4.87% , which are consistent with the theoretical calculation.

The simulation and experiment shows that with the influence of the unbalanced mass, the rotor vibrates when the rotor speed is fixed. However, after the thermal deformation, the clearance change leads to the axis orbit expand both in the top and bottom AMB. The thermal deformation will reduce the performance of the AMB controller and affect the unbalanced response of the AMB-rotor system. The experiment shows that the thermal deformations affect the clearance, and then reduce the performance of the AMB controller and affect the unbalanced response of the AMB-rotor system. This is consistent with theoretical analysis and simulation.

The influence of the clearance changing on the electromagnetic force, AMB stiffness and transducer measurement is discussed with the theoretical electromagnetic calculations, including the AMB force, transducer and eddy current. The theoretical calculations in this paper has general applications in the controller improvement of the AMBs under clearance change and provides a reference for mechanical structure design and controller design of AMBs.

ACKNOWLEDGMENT

This paper is financially supported by the National Science and Technology Major Project of China (2011ZX069) and Project 61305065 supported by NSFC.

REFERENCES

- [1] Z. Zhang, Z. Wu, Y. Sun, and F. Li, "Design aspects of the Chinese modular high-temperature gas-cooled reactor HTR-PM," *Nuclear Engineering and Design*, vol. 236, no. 5-6, pp. 485-490, Mar. 2006.
- [2] Z. Zhang and Y. Sun, "Economic potential of modular reactor nuclear power plants based on the Chinese HTR-PM project," *Nuclear Engineering & Design*, vol. 237, no. 23, pp. 2265-2274, Dec. 2007.
- [3] G. Yang, Z. Shi, N. Mo, and L. Zhao, "Research on active magnetic bearing applied in Chinese modular high-temperature gas-cooled reactor," *Progress in Nuclear Energy*, vol. 77, pp. 352-360, Nov. 2014.
- [4] G. Yang, Z. Shi, and N. Mo, "Technical design and engineering prototype experiment of active magnetic bearing for helium blower of HTR-PM," *Annals of Nuclear Energy*, vol. 71, pp. 103-110, Sep. 2014.
- [5] Z. Sun, Y. He, J. Zhao, Z. Shi, L. Zhao, and S. Yu, "Identification of active magnetic bearing system with a flexible rotor," *Mechanical Systems & Signal Processing*, vol. 49, no. 1-2, pp. 302-316, Dec. 2014.
- [6] Z. Sun, X. Yan, J. Zhao, X. Kang, G. Yang, and Z. Shi, "Dynamic behavior analysis of touchdown process in active magnetic bearing system based on a machine learning method," *Science & Technology of Nuclear Installations*, vol. 2017, no. 5, pp. 1-11, Oct. 2017.
- [7] C. Zhang, Z. Yi, and Z. Zhang, "THD Analysis of high speed heavily loaded journal bearings including thermal deformation, mass conserving cavitation, and turbulent effects," *Journal of Tribology*, vol. 122, no. 3, pp. 597-602, July 2000.
- [8] H. Suzuki, K. Urano, H. Kumehara, and K. Kusumoto, "Minimizing thermal deformation of ultraprecision machine tool induced by lubricating oil of hydrostatic bearings," *Journal of the Japan Society of Precision Engineering*, vol. 75, no. 9, pp. 1106-1111, Sep. 2009.
- [9] K. Jiang, C. Zhu, L. Chen, and X. Qiao, "Multi-DOF rotor model based measurement of stiffness and damping for active magnetic bearing using multi-frequency excitation," *Mechanical Systems & Signal Processing*, vol. 60-61, pp. 358-374, Aug. 2015.
- [10] J. I. Inayat-Hussain, "Nonlinear dynamics of a statically misaligned flexible rotor in active magnetic bearings," *Communications in Nonlinear Science & Numerical Simulation*, vol. 15, no. 3, pp. 764-777, Mar. 2010.
- [11] M. FeLix, A. LizaRraga, A. Islas, and A. Gonzalez, "Analysis of a ferrofluid core LVDT displacement sensor," *IECON 2010-36th Annual Conference on IEEE Industrial Electronics Society*, Glendale, AZ, 2010.
- [12] A. Hossain and M. J. Dwyer, "A new type of liquid density transducer based on the principle of linear variable differential transformer," *Sensors for Industry, 2001. Proceedings of the First ISA/IEEE Conference*, pp. 270-275, 2001.
- [13] J. Yu and L. Zhao, "Internal vibration source analysis of AMB-rotor system in HTR-PM primary helium circulator," *ASME International Conference on Nuclear Engineering*, London, 2018.
- [14] J. Tang, B. Xiang, and Y. Zhang, "Dynamic characteristics of the rotor in a magnetically suspended control moment gyroscope with active

magnetic bearing and passive magnetic bearing,” *ISA Trans*, vol. 53, no. 4, pp. 1357-1365, Nov. 2014.

- [15] Y. He, Z. Shi, L. Shi, and Z. Sun, “Unbalance compensation of a full scale test rig designed for htr-10gt: a frequency-domain approach based on iterative learning control,” *Science and Technology and Nuclear Installations*, vol. 2017, no. 1-15, Jan. 2017.
- [16] T. Fan, Z. Sun, X. Zhang, X. Yan, J. Zhao, and Z. Shi, “Residual unbalanced mass determination of an AMBs controlled rotor based on control current analysis of the feedback loop,” *ASME. International Conference on Nuclear Engineering*, London, vol. 1.



Zhe Sun is currently an Associate Professor and Ph.D. Supervisor of Tsinghua University. His research interests are control and monitoring of active magnetic levitation system, rotor dynamics, statistical learning theory and its engineering application, etc. He has published more than 20 SCI/EI index papers and 10 national patents. He presides over and participates in a series of National Science and Technology Major Project of China, National Natural Science Foundation of China and National High-tech Research and Development Program of China.



wheel system.

Jinpeng Yu received his B.Sc. degree in 2015 from Dalian University of Technology. Now he is studying for a Ph.D. in the Institute of Nuclear and New Energy Technology, Tsinghua University. He is mainly engaged in active magnetic bearing and its application in fly-